Exposure to ultraviolet radiation causes proteomic changes in embryos of the purple sea urchin, *Strongylocentrotus purpuratus*

Joseph P. Campanale [1], Lars Tomanek, Nikki L. Adams *

Biological Sciences Department, 1 Grand Avenue, California Polytechnic State University, San Luis Obispo, CA 93407, USA

We performed experiments to determine how environmentally relevant ultraviolet radiation (UVR) affects protein expression during early development in the sea urchin, *Strongylocentrotus purpuratus*. To model the protein-mediated cell cycle response to UV-irradiation, six batches of embryos were exposed to UVR, monitored for both delays in the first mitotic division and changes in the proteome at two specific developmental time points. Embryos were exposed to or protected from artificial UVR (11.5 W/m^2) for 25 or 60 min. These levels of UVR are within the range we have measured in coastal waters between 0.5 and 2 m. Embryos treated with UVR for 60 min cleaved an average of 23.2 min (±1.92 s.e.m.) after UV-protected embryos. Differential protein spot migration between UV-protected and UV-treated embryos was examined at 30 and 90 min post-fertilization using two-dimensional SDS-PAGE (2D GE). A total of 1306 protein spots were detected in all gels, including differences in 171 protein spots (13% of the detected proteome) in UV-treated embryos at 30 min post-fertilization and 187 spots (14%) at 90 min post-fertilization (2-way ANOVA, $P = 0.03$, $n = 6$). The majority of the proteins affected by UVR were subsequently identified using matrix assisted laser desorption ionization tandem time-of-flight mass spectrometry (MALDI-TOF–TOF MS). Our results indicate UVR affects proteins from multiple cellular pathways and indicate that the mechanisms involved in UV-stress and UV-induced developmental delay in sea urchin embryos are integrated among multiple pathways for cellular stress, protein turnover and translation, signal transduction, cytoskeletal dynamics, and general metabolism.

1. Introduction

Ultraviolet radiation (UVR, 290–400 nm) reaching Earth's surface can have severe physiological consequences and impact ecological distributions of organisms. Moreover, the anthropogenic release of ozone-depleting gasses for decades led to reductions in Earth's ozone layer, subsequently increasing the penetration of UVR into the oceans. Although the increases in UVR, particularly ultraviolet B (UVB, 280–320 nm) have been in polar regions, temperate latitudes have also experienced an increase in total UVR (Kerr and McElroy, 1993; Madronich et al., 1998; McKenzie et al., 2007; Smith et al., 1992; WMO, 2007). Atmospheric ozone levels are not expected to return to 1980-levels in polar regions until the year 2050. However, UVB levels may continue to increase a few percent per decade due to global climate change and increases in water clarity due to increased temperatures and decreased dissolved organic carbon (Anderson et al., 2001; Häder et al., 2007; Madronich et al., 1998; McKenzie et al., 2003, 2007; UNEPEEAP, 2004, 2005; WMO, 2007; Zepp et al., 2003). Therefore, developing a complete understanding of how UVR affects organisms and identifying strategies used by marine organisms to cope with exposure to UVR in marine environments, can shape the predicted ecological impacts of increased UVR in marine ecosystems.

Harmful levels of solar UVA (UVA, 321–400 nm) and UVB can penetrate several meters in organically rich coastal seawater of temperate regions (Adams et al., 2001; Smith and Baker, 1979; Tedetti and Sempere, 2006). Even at the pre-ozone depletion levels, UVR is deleterious to biochemical and physiological functioning by altering cellular targets including proteins, DNA, and lipids. Each of these molecules absorbs light differently and may vary in UV-sensitivity. For example, exposure to UVB results in direct protein damage by photochemical degradation of tryptophan and tyrosine residues (Hollósy, 2002) and damages DNA through the production of cyclobutane pyrimidine dimers (CPD's) among other photoproducts (Imlay and Linn, 1988; Lesser, 2010; Lesser et al., 2003, Peak and Peak, 1990; Setlow, 1974; Tevini, 1993). UVA causes photooxidative damage through the production of reactive oxygen species (ROS) that rapidly oxidize nucleic acids, proteins and lipids (Pourzand and Tyrell, 1999; Tyrrell, 1991), which have been documented in sea urchins (Lesser et al., 2006; Lesser, 2010; Lister et al., 2010). UV-induced injury to these molecules can affect the development and survivorship of marine

organisms as well as reduce the total productivity of phytoplankton and zooplankton (Cullen and Neale, 1994; Williamson et al., 1994) ultimately applying systemic pressure to aquatic ecosystems and altering trophic interactions (Caldwell et al., 1998; Häder et al., 2007).

Because development requires coordination of a greater number of cellular processes during a relatively short time period, embryos are thought to be the most sensitive life stage of aquatic organisms. Echinoid embryos in particular have been used extensively as a model for elucidating the effects of environmental factors such as temperature, oxidative stress, chemical pollutants and UVR (Adams and Shick, 1996, 2001; Anderson et al., 1993; Bancroft et al., 2007; Lesser et al., 2003; Lesser, 2010; Lister et al., 2010; Pesando et al., 2003; Russo et al., 2003). Specifically, exposure of eggs and early embryos to UVR causes delayed completion of the first mitotic division with embryos stalling at prophase (the most sensitive stage) in the cell cycle (Adams and Shick, 1996, 2001; Giese, 1964; Lamare and Hoffman, 2004; Rustad, 1971). These delays in development can result in longer planktonic periods that increase predation pressure and advection from adult settling sites (Jackson and Strathmann, 1981; Morgan and Christy, 1996; Strathmann et al., 2002). Moreover, multiple studies, including many *in situ* field studies, have shown that long-term exposure of sea urchin embryos to UVR damages biomolecules, results in an increased energy cost for the production of stress-response compounds, and increases abnormal development/morphogenesis, including mortality (Adams and Shick, 1996, 2001; Bonaventura et al., 2005, 2006; Isley et al., 2009; Lamare et al., 2007; Lesser, 2010; Lister et al., 2010).

Importantly, sea urchin embryos have a variety of cellular defense mechanisms to execute the developmental program during periods of stress. These include the evolution of a "be prepared" strategy, which involve selective packaging of defense molecules in embryos to combat environmental fluctuations in toxic chemicals, heavy metals and during periods of redox flux (Hamdoun and Epel, 2007). Some of these molecules include natural sunscreens such as mycosporine-like amino acids to absorb UVR (e.g. Adams and Shick, 1996, 2001), carotenoids (e.g. Lamare and Hoffman, 2004), antioxidative enzymes (e.g. Lesser, 2010) or repair enzymes such as photolyase (e.g. Isley et al., 2009; Lamare et al., 2006). Examples of other protein defenses include Cytochrome P450, heat-shock proteins (HSPs) and efflux transporters (Hamdoun and Epel, 2007). In addition, cellular stress responses (CSR) conserved in all organisms sense macromolecular damage and often lead to cell cycle delays (Kültz, 2005). All kingdoms studied to date appear to activate the CSR upon macromolecular damage during exposure to natural stressors including temperature, osmotic fluxuation and UV-irradiation (Kültz, 2005). Proteins affected by UVR and involved in either cleavage delay or the CSR in UV-stressed sea urchin embryos have not yet been comprehensively identified; thus, a proteomic analysis can reveal which proteins of the CSR are expressed in embryos and if they are changing in response to UVR. Furthermore identification of proteins in the CSR could provide further evidence identifying ubiquitous physiological and ecological biomarkers of UV-stress.

Proteomics, the study of global protein structure and function, has become an instrumental way to discover protein biomarkers of ecological stress in marine invertebrates (Hamer et al., 2004; Tomanek, 2005, 2011). In addition, the *Strongylocentrotus purpuratus* genome was sequenced and the embryonic transcriptome was described, facilitating more comprehensive proteomic studies (Samanta et al., 2006; Sodergren et al., 2006). The *S. purpuratus* genome-sequencing project provided information about the number of proteins that are in the sea urchin genomic arsenal for chemical defense, including those known to be important in responding to UV-induced oxidative stress in other organisms (Goldstone et al., 2006). Initial surveys provided insight for the potential regulation of basic sea urchin development in non-stressed conditions, but functional analysis, especially during stress have yet to be conducted (Bradham et al., 2006; Fernandez-Guerra et al., 2006; Goel and Mushegian, 2006; Howard-Ashby et al., 2006; Livingston et al., 2006).

In this study, we used a comparative proteomic survey of UV-exposed and UV-protected sea urchin embryos at two specific developmental time points to provide one of the first descriptions of how UVR can affect protein abundance, either due to changes in expression, post-translational modification or degradation of proteins in multiple cellular pathways simultaneously. This report utilizes the insights from the *S. purpuratus* genome to identify how the majority of the early sea urchin embryonic proteome responds to non-lethal but stressful doses of UVR and begins to resolve the long-standing question of what proteins and cellular pathways are altered during UV-induced cell cycle delays.

2. Materials and methods

2.1. Sea urchin collection, gamete gathering and embryo culture

Adult *Strongylocentrotus purpuratus* were collected from Goleta, California in November 2007 and held at 10 °C in re-circulating seawater aquaria. Sea urchins were induced to spawn using intracoelomic injections of 0.55 M KCl. Eggs from six females were collected separately in 0.22 μm filtered seawater (FSW), diluted to 5% (v/v), and treated with 1 mM ammonium triazole (ATAZ) to prevent crosslinking of the fertilization envelopes. Eggs were fertilized using a 1:50,000 dilution of dry sperm from a single male and embryos were cultured in FSW between 13 and 15 °C during UVR exposure. All cultures achieved at least 95% fertilization.

2.2. UVR-exposure and quantification

Batches of embryos ($n = 6$) were divided into two aliquots that were either exposed to or protected from artificial UVR using UVA-340 lamps (Q-Panel Lab Products, Cleveland, OH, USA) that simulate the solar spectrum of UVR (as in Adams and Shick, 2001; Shick et al., 1999). Embryos were exposed to photosynthetically active radiation (PAR, 400–700 nm, UV-protected) using UV-opaque acrylic cover (Plexiglas UF3, Arkema, Philadelphia, PA, USA, 50% cutoff at 400 nm), or PAR + UVA + UVB (295–700 nm, UV-treated) using UV-transparent acrylic cover (Plexiglas G-UVT, Arkema, 50% cutoff at 290 nm) over glass Petri dishes containing a monolayer of embryos.

UVA and UVB irradiance was measured during UVR exposures using an IL 1400A radiometer coupled with a UVA sensor (model SEL033) or UVB sensor (model SEL240) that have maximal peak sensitivities at 350 nm and 295 nm respectively (International Light, Newburyport, MA, USA). Average measured UVA-irradiance was 11.1 W/m^2 (±0.2 s.e.m.) and UVB-irradiance was 0.4 W/m^2 (±0.01 s.e.m.). These irradiances were selected because they were within the average range of UVA and UVB irradiances we have measured between 0.5 and 2 m in the coastal waters at our Center for Coastal Marine Sciences pier in San Luis Obispo Bay (Adams, unpublished).

Embryos were exposed to UVR for either 25 min ("30 min" samples, see below) or 60 min (known to cause cleavage delay but not death as per Adams (unpublished), "90 min" samples, see below) after fertilization. Embryos exposed to UVR for 25 min experienced cumulative UVA and

UVB doses of 16.62 kJ/m^2 and 0.60 kJ/m^2 respectively. Embryos exposed to UVR for 60 min experienced cumulative UVA and UVB doses of 39.90 kJ/m^2 and 1.43 kJ/m^2 respectively. UV-exposure experiments included PAR illumination to allow photorepair in UV-exposed embryos.

2.3. Developmental delay assays

Embryos from each batch were preserved in 1% formalin buffered FSW every 10 min post-fertilization until completion of mitosis. At least, 200 embryos from each sample were scored for cell division and the percentage of cleaved embryos was calculated. A random complete block design (RCBD) ANOVA was performed to assess effects of UV-treatment on the timing of development to 50% of each batch to complete cleavage for factors of UV-treatment and blocked by batch of eggs. The degree of UV-induced delay in division for all six batches of embryos was determined and percentage cleavage delay (PCD) was calculated for each batch as per Adams and Shick (1996) using the following equation:

$$\mathrm{PCD} = \frac{\text{Time for 50\% } (T_{50}) \text{of UV} - \text{treated embryos to divide} - T_{50} \text{ of UV} - \text{protected embryos to divide}}{T_{50} \text{ of UV} - \text{protected embryos to divide}}$$

2.4. Protein lysate preparation and quantification

In parallel, lysates were prepared at 30 min and 90 min. Embryos were sampled at 30 min post-fertilization because irradiation of sea urchin eggs and early embryos prior to 30 min post-fertilization results in developmental retardation, but does not affect DNA synthesis (Adams, unpublished; Rao and Hindgardner, 1965; Zeitz et al., 1968). Lysates were also prepared at 90 min post-fertilization just prior to the onset of mitosis in UV-protected embryos. Embryos were lysed on ice using a 27 G needle in a buffer containing 0.1% Triton X-100, 15 mM disodium EGTA, 150 mM NaCl, 20 mM HEPES pH 7.0, 60 mM β-glycerolphosphate, 0.5 mM Na_2VO_4, 1 mM NaF, Roche CompleteMini PIC. Lysates were centrifuged at 14,000 rpm and immediately snap frozen in liquid nitrogen and stored at −80 °C until analysis. Protein concentrations were determined using the BCA method (Pierce Biotechnology, Rockford, IL, USA).

2.5. Two-dimensional gel electrophoresis

A total of 100 μg of protein was denatured in DeStreak Rehydration Solution (GE Healthcare, Piscataway, NJ, USA) and passively rehydrated into pH 4–7 isoelectric focusing (IEF) strips (GE Healthcare). First dimension isoelectric focusing of proteins was performed for 21.8 kilovolt hours on a GE Healthcare Ettan IPGphor3 IEF System. Strips were equilibrated first in a 1% DTT/equilibration buffer (6 M urea, 75 mM Tris HCl, 29.3% glycerol, 2% SDS, 0.002% bromophenol blue) and then in a 4% Iodoacetamide/equilibration buffer. Proteins were separated by molecular weight using 10% SDS-PAGE on a BioRad (Hercules, CA, USA) Criterion Dodeca system. One gel was run for each batch of embryos for each treatment at each time-point (six batches of embryos, two UV-treatments at two time-points for a total of 24 gels). To minimize gel-to-gel variation between UVR treatments of the same batch of embryos, 2D GE for all 30 min UVR treated and protected lysates and all 90 min lysates were run simultaneously in the first and second dimension. Preliminary analysis of protein spots from triplicate gels from the same lysate for each time point demonstrated that more spots varied between treatments than among these gels (data not shown).

2.6. Protein detection and image analysis

Proteins in gels were fixed in 7% glacial acetic acid/50% methanol and stained with SYPRO Ruby stain (Invitrogen, Carlsbad, CA, USA). Proteins were detected using a Typhoon Trio + Imager (GE Healthcare, Piscataway, NJ, USA) at 525 pmt voltage and a laser path of 50 μm. All gel images were warped to a composite image (proteome map), which was used to detect spots that were subsequently found in the original gel images using Delta2D software (version 4.0, Decodon GmbH, Greifswald, Germany), as described in Berth et al. (2007). Spot boundaries for all spots were designated on the master proteome map and because the total proteome map was a compilation of all 24 gel images, it offered the advantage of accurate spot detection and quantification across all raw gel images. Spot intensities were quantified as pixel density, which were normalized within each gel image against the total sum of pixel densities from all spots to quantify the percent volume of each spot. The percent volume represented spot expression density and was used to compare protein spots across gel images. Further, a fusion image was compiled digitally to create a visual representation of all six batches for each time point at each UV-treatment.

Differential normalized spot densities were analyzed using the The Institute for Genomic Research Multi Experiment Viewer software (TIGR MeV, version 4.0, see Saeed et al., 2003). A 2-way ANOVA for each spot was performed to identify significant differences in protein expression between UV-treatments and among individual batches for each time point at $P \leq 0.03$. An $\alpha \leq 0.03$ was selected to reduce the number of false spots showing differential regulation by UVR. Although the statistical power to analyze the differences between time points existed using this experimental design, a 3-way ANOVA could not be performed in the TIGR MeV software to remove any significant effect of individual batch. Delta2D software doesn't allow for analysis of covariance of spots between gel images. Furthermore, comparisons between the 30 and 90-minute time points were not performed because of the differences in total UVR dose between the two time points. For these reasons the analysis was limited to a 2-way ANOVA for factors of UV-treatment and blocked by the factor of individual batch of sea urchin embryos at each time point.

2.7. Matrix assisted laser desorption ionization-tandem time of flight mass spectrometry

Protein spots that differed between UV-treatments were excised from gels using a BioRad ProteomeWorks automated spot picker from two different 2D gels. Each spot was digested with 82 ng of trypsin (Promega, Madison WI, USA) and the resulting peptide fragments were spotted on an Anchorchip metal target (Bruker Daltonics Inc.) using α-cyano-4-hydroxycinnamic acid (HCCA). Matrix assisted laser desorption ionization-tandem time of flight mass spectrometry (MALDI-TOF–TOF MS, Ultraflex II, Bruker Daltonics Inc., Billerica, MA, USA) was used to identify proteins. Tandem mass spectrometry (MS/MS) was performed on at least four of the most abundant peaks found in the original mass spectrum (MS).

To confirm spot identities, spectra were analyzed using the Biotools software suite (version 3.1, Bruker Daltonics Inc.). Resulting peptide fragment molecular weights from both the MS and MS/MS were then searched against an in-house database created using MASCOT software (www.matrixsciences.com) containing all known sequences from *S. purpuratus* (obtained from NCBI in January 2009). Searches were performed using the MOlecular Weight SEarch (MOWSE) method modified by MASCOT (see Perkins et al., 1999). All identifications represent significant MASCOT MOWSE scores set at a threshold of ≤0.05. Expression volumes for all protein spots identified by mass spectrometry were standardized for each spot across all batches of embryos. Both standardized protein spot expression density and embryo batch were hierarchically clustered using Pearson's correlation metric. Support for clustering protein expression patterns was analyzed by bootstrap analysis.

2.8. Functional classification of proteins

Functional classification of identified proteins was conducted initially using the NCBI Conserved Domain Database (CDD, Marchler-Bauer et al., 2009) to identify clusters of eukaryotic orthologous groups (KOGs). This database search tool allowed for the identification of 20 KOG groupings and provided protein family information. CDD analysis was followed with a survey of the current literature.

3. Results

3.1. Effects of UVR on mitosis

S. purpuratus embryos vary in sensitivity to UVR across time during the first cell division (Adams personal observation; Rustad, 1960), therefore we examined the UV-induced changes in protein expression at two time points representing two distinct events during early development. At 30 min post-fertilization, the "sweep" of proteins transitioning the oocyte to an embryo has likely occurred (Roux et al., 2008; Stitzel and Seydoux, 2007) and includes resumption of DNA synthesis in both pronuclei, regardless of UV-treatment (Rao and Hindgardner, 1965; Zeitz et al., 1968). At 90 min post-fertilization, the UV-protected embryos begin to undergo cleavage while the UV-treated embryos stall at the morphologically distinct streak stage in prophase (Adams personal observation; Rustad, 1971), where cells are most highly sensitive to UVR.

As expected (c.f. Adams and Shick, 1996), moderate, ecologically relevant UV-treatment resulted in delayed cleavage for all batches of embryos after a 60 min UVR exposure ($\bar{x} = 23.24$ min ± 1.92 s.e.m., Fig. 1). The time for 50% of the embryos to divide was significantly delayed by UV-treatment ($P < 0.0001$) and varied significantly by batch ($P = 0.031$). There was no interaction between UVR treatment and embryo batch, and UV-treatment resulted in delayed cleavage for all batches. Fifty percent of UV-protected embryos cleaved between 110 min and 122 min, whereas 50% of embryos from the same batches treated with a 41.31 kJ/m^2 cumulative dose of UVR cleaved between 133 min and 154 min.

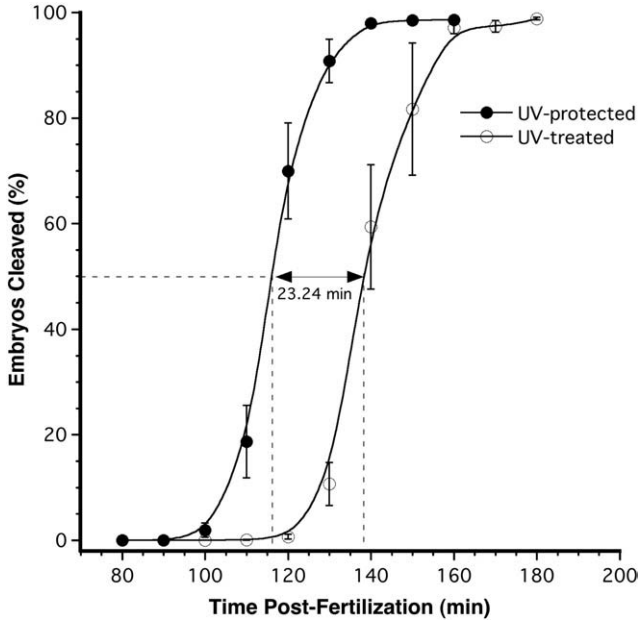

Fig. 1. Graph of mean (±s.e.m.) cleavage rates from UV-protected and UV-treated *S. purpuratus* embryos (n = 6 batches) at 10 min intervals starting at 80 min post-fertilization through the completion of the first mitotic cell cycle (n = 200 embryos counted for each batch for each time point). Embryos were UV-treated (○) or UV-protected (●) from a total dose of 41.31 kJ/m^2 UVR (290–400 nm) delivered over a period of 60 min. Smooth curves were fit to data points (black lines) and dashed lines identify the average time required for 50% of embryos to cleave for each treatment. ↔ indicates the average UV-induced delay in cleavage to be 23.24 min.

Batches of embryos, on average, suffered a 19.93% (±1.53 s.e.m.) UV-induced delay in mitosis. The remaining UV-protected and UV-treated batches of embryos were cultured at 15 °C. Although mortality was not assessed directly, all batches of embryos from both UV-treatments were at the swimming hatched blastula stage within 24 h post-treatment and no morphological differences were detected.

3.2. Differential spot migration

Fig. 2A and B display color overlaid average proteome maps of the 30 min and 90 min post-fertilization samples. Using the total fusion proteome map described above, 1306 spot boundaries were established. These overlays were not analyzed specifically because even though great care and effort was taken to minimize incorporating experimental errors in UVR treatment, lysate preparation, creation of the 2D gels and image warping, these are average images from embryos developing at slightly different rates. Creating total and time point specific image fusions rather served as reference gel images to depict the results of statistical analyses by providing a single image of all batches at all UV-treatments for each time point.

At least 171 protein spots (13% of the total proteome) showed differential spot volumes across each batch of embryos for UV-treatment at 30 min post-fertilization (2-way ANOVA for each normalized spot for each individual and treatment, ≤0.03). At 90 min post-fertilization, a total of 187 spots (14% of the proteome) showed differential spot volumes between UV-treated and UV-protected batches of embryos. Blocking by batch ensured that the most consistent spots among batches that migrated differently due to UV-irradiation were identified.

At this time, it is not possible to distinguish whether differential protein spot migration of proteins is a result of direct UVR damage, protein turnover, new translation, or a result of post-translational modification (PTM), or extracellular efflux. Therefore, any spot exhibiting differential migration is broadly referred to as being differentially regulated.

3.3. MALDI-TOF–TOF protein identifications

First, the protein spots that were significantly differentially regulated between UV-treatments were selected for MS analysis. Second, spots also had to be abundant enough (>0.005% volume in raw 2D images) for high quality MS/MS spectra on at least the four of the most abundant fragments found in the MS spectrum. A total of 176 protein spots were selected for identification, 94 spots for 30 min and

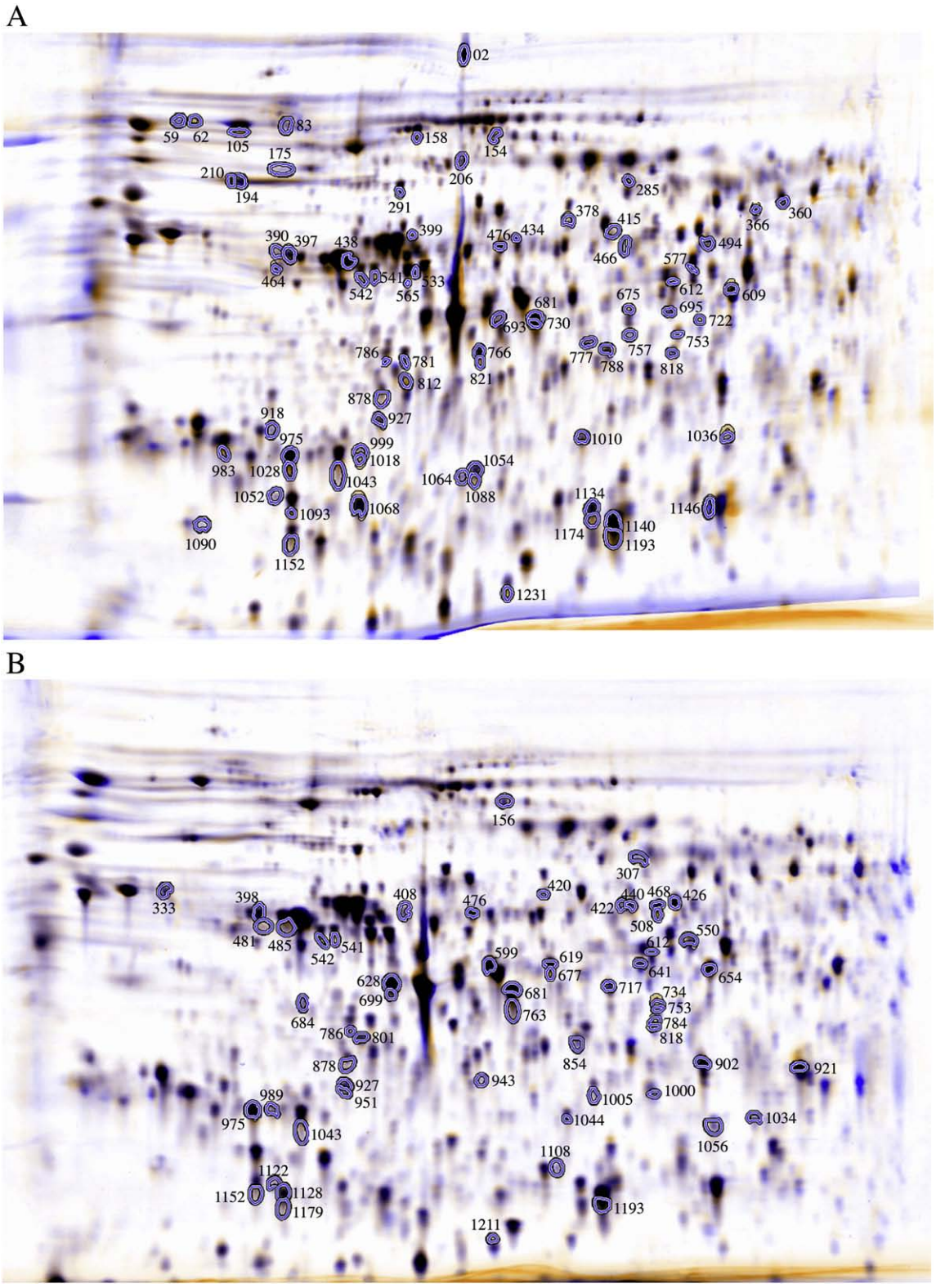

Fig. 2. Overlay of fusion averaged 2D gel images (proteome maps) for six batches of *S. purpuratus* embryos. Colored spots represent proteins from lysates from different UVR treatments [UV-protected (blue), UV-treated (orange) and overlap (black)]. Highlighted and numbered protein spots correspond to Table 1 as spots that migrate differently due to UVR treatment and identified by MALDI-TOF MS + MS/MS. Overlay of proteome profiles for (A) Embryos at 30 min post-fertilization either protected from or exposed to a total of 17.21 kJ/m^2 UVR (n = 12 gels, 6 for each UV-treatment) and (B) Embryos at 90 min post-fertilization either protected from or exposed to a total of 41.31 kJ/m^2 UVR. Each overlay contains 12 2D gel images per time point. All six batches are represented in each treatment at each time point in both A and B.

82 spots for 90 min post-fertilization. All but 46 protein spots were identified using the minimum threshold of a significant MOWSE score for combined MS and MS/MS spectra searched against the predicted *S. purpuratus* proteome ($P<0.05$, Fig. 2A and B, Table 1). Proteins identified by MS + MS/MS are outlined and labeled in Fig. 2A and B and numbers associated with each spot relate to the identifications in

Table 1
MS + MS/MS identification of proteins with altered migration after UVR exposure of *S. purpuratus* embryos grouped by KOGs.

Time (min)[a]	Protein identification	Spot number[b]	NCBI accession	Relative fold change[c]	KOG[d]
Amino acid transport and metabolism					
30	Glutamine synthetase, isoform 2	730, 693, 681	XP_801741.2	1.3, −1.17, −1.37	683
90	Glutamine synthetase, isoform 2	763, 681	XP_801741.2	1.42, −1.33	683
	Hypotheical protein	1108	XP_783660.1	−1.54	1709
	Serine hydroxymethyl transferase	398	XP_001176829.1	−1.09	2467
Carbohydrate transport and metabolism					
30	Adenosine kinase A, isoform 1	781, 786	XP_780906.2	1.62, 1.75	2854
	Fructose-1,6-bisphosphatase 1	788	XP_793452.2	−1.19	1458
	Gk2-prov protein, partial	434	XP_785650.2	2.02	2517
90	Adenosine kinase A, isoform 1	801	XP_780906.2	−1.21	2854
	Fumarylacetoacetase	677, 619	XP_787535.2	1.66, −1.41	2843
	Transaldolase	943	XP_792583.2	−1.33	2772
	UDP-glucose dehydrogenase	440	XP_784861.1	−1.25	2666
Cell cycle control, cell division, chromosome partitioning, cytoskeleton					
30	MGC143070 (Calponin domain)	927	XP_001191889.1	−1.14	3000
	Translationally controlled tumor protein	1068	XP_795619.2	1.20	1727
90	Hypothetical protein (microtubule binding/cell cycle progression)	951	XP_787950.1	1.19	3000
	MGC143070 protein, partial (Calponin homology)	927	XP_001191889.1	−1.18	3000
Cell wall/membrane/envelope biogenesis					
90	30 kDa yolk granule protein YP30	1005	XP_781365.1	1.09	1437
	Hypothetical protein (UTP-glucose-1-phosphate uridylyltransferase)	420	XP_779933.2	−1.29	2388
Chromatin structure and dynamics					
30	Retinoblastoma binding protein 4 variant isoform 2	397	XP_801904.1	−1.15	264
Coenzyme transport and metabolism					
90	Adenosylhomocysteinase	550	XP_780172.1	1.46	1370
	Hypothetical protein	786	XP_784275.1	1.47	1540
Cytoskeleton					
30	Actin CyIIIb	2	NP_999692.1	−2.72	676
	Beta tubulin	438	XP_791790.1	1.80	1375
	CG10540-PA (F-actin capping protein)	1010	XP_001176707.1	−1.34	836
	CG8649-PC (Calponin homology)	291	XP_001181286.1	1.93	46
	Gelsolin	609,565	XP_001176123.1	1.96, −1.47	443
	SUArp3 isoform 1	577	XP_780265.1	1.43	678
	Tropomyosin	918	XP_781599.1	−1.36	1003
	Tubulin, alpha 2, isoform 2	399	XP_001178868.1	1.76	1376
90	Actin CyIIb	628	NP_999693.1	−1.11	676
	Actin CyIIIb	699	NP_999692.1	1.51	676
	Beta tubulin	485	XP_791790.1	1.51	1375
	CG10540-PA (F-actin capping protein)	1044	XP_001176707.1	−1.27	836
	Gelsolin	641, 654	XP_001176123.1	1.23, −1.27	443
Energy production and conversion					
30	ENSANGP00000027279, partial	812	XP_793193.2	2.38	1626
	Isocitrate dehydrogenase 2 (NADP+), mitochondrial	695	XP_001176537.1	−1.52	1526
90	Cytosolic malate dehydrogenase	921	XP_796283.1	−1.72	1496
	GA10614-PA (ATP synthase E/31 kDa)	1000	XP_001203960.1	−1.77	1664
Extracellular structures					
30	PTK9L protein tyrosine kinase 9-like	818	XP_793525.1	−1.58	1747
90	PTK9L protein tyrosine kinase 9-like	784, 818	XP_793525.1	1.58, −1.74	1747
General function prediction					
30	CG7820-PA (Carbonic anhydrase)	1036	XP_782997.2	1.55	382
	Nuclear matrix protein NMP200	366	XP_001204254.1	1.96	289
90	CG7820-PA (Carbonic anhydrase)	1056	XP_782997.2	−1.17	382
	Translin	1034	XP_781342.2	−1.39	3067
Lipid transport and metabolism					
30	Apolipoprotein B	466	XP_800206.2	−2.41	4338
	Hydroxymethylglutaryl-CoA synthase, cytoplasmic	476	XP_801879.1	−1.23	1393
90	Hydroxymethylglutaryl-CoA synthase, cytoplasmic	476	XP_801879.1	−1.30	1393
Nuclear Structure					
30	Hypothetical protein	415	XP_793278.2	1.68	2086
Nucleotide transport and metabolism					
30	Bisphosphate nucleotidase	777	XP_785239.1	−1.26	3099
	IMP cyclohydrolase	360	XP_793444.1	−1.26	2555
	Intermediate Chain	62, 59	XP_786989.1	1.87, −1.82	888

(continued on next page)

Table 1 (*continued*)

Time (min)[a]	Protein identification	Spot number[b]	NCBI accession	Relative fold change[c]	KOG[d]
Posttranslational modification, protein turnover, chaperones					
30	14-3-3 like protein 2	1018, 999, 1043	XP_780530.1	1.414, −1.34, 1.77	841
	1433_CANAL 14-3-3 protein homolog isoform 1	1028, 975	XP_780278.1	1.763, −1.14	841
	26S proteasome subunit p44.5	612	XP_792957.1	−1.31	1463
	Glutathione peroxidase, partial	1146	XP_784500.2	−3.73	854
	HS1 (14-3-3 family)	1093, 1052	XP_788276.1	1.55, −1.30	841
	HSP70 isoform 3	210, 194	XP_802057.1	1.82, −1.33	100
	Hypothetical protein (Chaperonin superfamily)	378	XP_785987.2	1.35	363
	Hypothetical protein (Proteasome alpha type 3)	1088, 1054	XP_796247.2	1.47, −1.61	184
	Peptidylprolyl isomerase D (Cyclophilin D)	675	XP_001201326.1	2.49	546
	Proteasome 26S subunit, non-ATPase, 13 partial	821, 766	XP_001181294.1	1.80, −1.17	2908
	Proteasome subunit, beta type 6, partial	1231	XP_001184184.1	2.74	174
	Proteasome alpha 2 subunit	1174, 1134	XP_001199987.1	1.632, −1.38	181
	Proteasome alpha 5 subunit	1152	XP_782337.1	1.38	176
	S-crystallin SL11 (major lens polypeptide), partial	1193, 1140	XP_001183993.1	2.14, −1.18	1695
	Thimet oligopeptidase 1	175	XP_790202.2	−1.61	2089
	Thioredoxin family Trp26	1064	XP_781152.1	−1.54	1730
	Valosin containing protein isoform 2, partial	158	XP_801708.2	2.40	730
90	14-3-3 like protein 2	1043	XP_780530.1	1.69	841
	1433_CANAL 14-3-3 protein homolog isoform 1	989, 975	XP_780278.1	−1.34, −1.20	841
	26S proteasome subunit p44.5	612	XP_792957.1	1.44	1463
	Chaperonin containing TCP, subunit 5	426	XP_801706.1	−1.23	357
	GDP-dissociation inhibitor isoform 1	408	XP_780206.2	−1.23	1439
	Hypothetical protein (GDP-fucose protein O-fucosyltransferase)	684	XP_001176732.1	−1.27	3849
	Peptidylprolyl isomerase D (cyclophilin D)	753	XP_001201326.1	−1.85	546
	Proteasome (prosome, macropain) subunit, beta type, 6, partial	1211	XP_001184184.1	3.87	174
	Proteasome alphs 5 subunit	1152	XP_782337.1	1.70	176
	S-crystallin SL11 (major lens polypeptide), partial	1193	XP_001183993.1	1.44	1695
Replication, recombination and repair					
90	Chain A, Structure of DNA repair protein Hhr23a isoform 1	333	XP_001176797.1	−1.43	11
RNA processing and modification					
30	GA10247-PA	494	XP_001191771.1	−1.30	4205
	Nucleolin	105	XP_797746.2	2.06	123
	Vasa homolog	154	XP_781494.2	1.27	335
90	GA10247-PA	422	XP_001191771.1	−1.58	4205
	Vasa homolog	156	XP_781494.2	1.12	335
Signal transduction mechanisms					
90	MGC79770 protein (Rho GDP dissociation inhibitor domain)	1179, 1122, 1128	XP_781627.1	1.26, 1.25, −1.08	3205
Transcription					
30	RuvB-like 2	533	XP_001184189	−1.45	2680
Translation, ribosomal structure and biogenesis					
30	34/67 kDa laminin binding protein	464	XP_792396.2	−1.67	830
	Eukaryotic translation initiation factor 2, subunit 1 alpha	878	XP_779939.1	1.21	2916
	G1 to S phase transition 1	206	XP_785469.2	−1.24	459
	Hypothetical protein (RPA2_OBF_family), partial	285	XP_001201004.1	1.58	556
	Initiation factor 4AII isoform 11	542, 541	NP_001091916	1.77, 1.65	328
	Translation elongation factor 1B alpha subunit isoform 1	893	XP_780033.1	1.55	1668
	Translation initiation factor eIF6	1090	XP_785113.1	−1.72	3185
90	34/67 kDa laminin binding protein	481	XP_792396.2	1.64	830
	Eukaryotic translation initiation factor 2, subunit 1 alpha	878	XP_779939.1	1.26	2916
	Eukaryotic translation initiation factor 3, subunit 2 beta, partial	854	XP_001193565.1	−1.16	643
	Hypothetical protein (RPA2_OBF_family), partial	307	XP_001201004.1	−1.25	556
	Initiation factor 4AII isoform 11	541, 542	NP_001091916.1	2.01, 1.66	328
	L10e/P0 (acidic ribosomal protein)	902	XP_794024.1	−1.29	815
Other					
30	GTP-binding protein	83	NP_999645.1	−1.22	none
	Hypothetical protein	722, 753, 757	XP_783181.2	3.90, −2.91, −1.67	none
90	Fascin	508, 468	NP_999701.1	1.69, −1.50	none
	Hypothetical protein	734, 717	XP_783181.2	2.19, −1.27	none

[a] Time point post-fertilization that protein was identified.
[b] Arbitrary spot number supplied by Delta 2D. Numbers correspond to numbers in Fig. 2A,B and Fig. 3A,B.
[c] Ratio of average spot normalized volume (treatment/control). Positive values represent an increase in spot volume for UV-treated samples. Negative values represent a decrease in spot volume for UV-treated samples.
[d] Cluster of Orthologous Groups of proteins (Tatusov et al., 2003).

Table 1. Furthermore, the average relative fold-change in spot volume (an average of all normalized spot volumes from the UV-treated batches divided by that of the same spot from the UV-protected batches) between UV-treated and -protected lysates is designated. These data identify the amount of average protein spot change occurring after UV-treatment and possibly reveal the degree of

sensitivity to UVR or differences in regulation during the developmental program.

By using the proteome map to set the spot boundaries first and then transferring these to all spots on all gel images second, spot consistency among gel images was accurately maintained among all combinations of raw 2D gels. In many cases, the same spot number across gels resulted in identical protein identifications. Also, identical protein identifications were made for different spot numbers between the treatments and among the time points. This shows highly repeatable and reliable identifications using MALDI-TOF–TOF to identify *S. purpuratus* proteins that are tracked as a protein spot shifting between the UV-protected or UV-treated gels. For example at 30 min post-fertilization, spot number 210 exhibited elevated expression in UV-protected lysates and spot number 194 had elevated expression in the UV-treated lysates. Both of these spots were identified as HSP70. Also, spot number 1043, which was identified as 14-3-3 protein homolog 2, was identified multiple times from multiple gels and therefore showed complex regulation within the UV-protected 2D gels at 30 min and 90 min post-fertilization (Fig. 2).

3.4. Protein expression density clustering

Standardized expression volumes for all protein spots identified by mass spectrometry across all batches of embryos are represented in a map of expression density (Fig. 3). Both standardized protein spot expression density and embryo batch were hierarchically clustered in rows and columns respectively by Pearson's correlation metrics. This figure compares expression density for identified spots across all gels. A significant bootstrap value of 100 confirmed two main clusters of proteins highlighted along the left of the map. These two clusters represent standardized expression of elevated and decreased protein spot abundances by all batches of embryos for the same treatment. Protein identifications for each spot are listed along the right of each row.

The hierarchical clustering of samples by UV-treatment across the top of the figure demonstrates robust analysis of the identified proteins and implicates these proteins as being affected by UVR (Fig. 3). All proteins that show statistical differences in spot abundance between treatments also show distinct expression patterns between UV-treatments. For example, the top row of the expression density map for 30 min post-fertilization indicates higher expression of a GTP-binding protein in all UV-protected batches, while the last row shows higher expression volumes of Vasa homolog protein in all UV-treated batches of embryos.

UV-treatment correlates strongly with protein spot expression levels (Fig. 3). Protein spots have either higher or lower spot expression density as indicated by the two clusters. The standardized expression values for all identified proteins across treatments were consistent in that a spot changing in expression density due to UVR had similar standardized values among batches and between UV-treatments. Only the two clusters of proteins were found among embryos exposed to UVR, indicating that all identified proteins have similar relative expression characteristics in response to UVR. Fig. 3 shows sub-clustering of protein expression, but we were not able to resolve meaningful differences below the two main clusters using hierarchical clustering.

3.5. Functional protein classifications

All identified proteins fit broadly into several categories for molecular function and showed varying trends in expression due to UV-treatment: (1) stress/repair and cellular metabolism; (2) protein translation; (3) cytoskeleton and cytoskeleton regulating proteins; (4) signal transduction; (5) protein turnover and degradation; (6) other (see Table 1). The most prominent of these proteins will be identified and compared in the discussion section. Proteins from each of these classes have the potential for being a sensitive biomarker of UV-stress. Furthermore, these proteins may be setting the physiological and ecological tolerances of planktonic embryos to UVR.

4. Discussion

This study examined effects of environmentally-relevant UVR on cell division and the proteome of *S. purpuratus* to identify how current levels of UVR may potentially affect the overall physiological response of marine organisms, especially broadcast spawned embryos, to stress in their environment. Most studies examining effects of UVR and stress responses of marine invertebrates focus on DNA damage or a single protein to understand how this may eventually affect the whole organism. In contrast and in an attempt to better understand the holistic response to UV-induced stress, we have documented changes to proteins involved in many pathways that control development, cell structure, stress responses, movement etc, all of which contribute to the activities and future fate of these embryos in the ecosystem. We present the most likely protein targets (in the PI range of 4–7) affected by UVR during the first mitotic phase of sea urchin development using a proteomic approach (Table 1). Where possible, we have attempted to understand and acknowledge how these changes in proteins may be linked to upstream damage to DNA. To our knowledge, this study provides some of the first evidence demonstrating that multiple proteins and cellular pathways are affected simultaneously by UV-irradiation or the mitotic delay it causes. Furthermore, our results reveal many candidate protein biomarkers of UV-stress for planktonic life stages of marine organisms.

4.1. Effects of UVR on mitosis and development

Our results confirm that ecologically relevant doses of UVR, cause developmental delays in *S. purpuratus* similar to other species of sea urchins (Fig. 1, Adams and Shick, 1996, 2001; Giese, 1964; Lamare and Hoffman, 2004; Lesser et al., 2003; Lesser, 2010). We observed an average UV-induced developmental delay of nearly 20% for the first cell cycle using UV-doses similar to those found in coastal regions of mid-latitude oceans recorded by our lab and others (Adams, unpublished; Lesser, 2010). Long-term exposure of embryos to these levels and wavelengths of UVR can lead to gross morphological abnormalities and death (Adams and Shick, 2001). This is particularly important because many species of marine invertebrates release their gametes, embryos and larvae into coastal waters. Early life stages face multiple sources of physiological stress such as extreme or variable temperatures and salinities, ocean acidification, low dissolved oxygen, pollution, and UVR. Only a few may survive long enough to settle and recruit to suitable habitats and become adults (e.g. Hoegh-Guldberg et al., 2008; Pechenik, 1987; Przeslawski, 2005). Importantly, delays in cell division allow time to repair UV-induced DNA and cellular damage. Nevertheless, delays in development can increase mortality both directly and indirectly by increasing the time spent in the plankton, increasing the probability of predation, physical stress, advection from adult habitats and starvation (Pechenik, 1987).

4.2. Proteomic analysis

Comparative proteomic analyses can uncover the molecular underpinnings controlling physiological responses to fluctuations in environmental conditions (Tomanek, 2010, 2011). Our comparative analysis of different proteome profiles demonstrates that UV-irradiation of sea urchin embryos causes changes in at least 176 proteins during the first cell cycle. Hierarchical clustering and the creation of protein expression density maps revealed that UVR directly or indirectly (via cell cycle delay) elevates expression of protein spots while simultaneously depressing expression of others

(e.g. Nucleolin and G1 to S phase transition protein respectively; Figs. 2, 3, Table 1). We interpret shifts in migration patterns of protein spots to be changes in translation, post-translational modifications or degradation rather than changes in transcription, because sea urchin embryos rely almost entirely on maternal reserves of mRNA and proteins until the blastula stage. Moreover, we found several different spots, sharing the same protein identification which may represent a subset of proteins in altered cellular signaling pathways during UV-induced stress (Table 1, Figs. 2, 3). Our data do not reconcile whether protein spots shifted due to UVR directly or indirectly. Nevertheless, they can provide a general view of how environmental stressors such as UVR affect the overall regulation of proteins.

4.3. Proteins potentially involved in UVR induced mitotic delay

The molecular basis of stress-induced cell cycle delays has been studied in many organisms. Several proteins identified in our study, including 14-3-3 protein, HSP70, Cyclophilin D, Glutathione peroxidase, 26S proteasome proteins, Isocitrate dehydrogenase, Thioredoxin and the nucleotide excision repair protein Rad23 (Hhr23), are consistent with those described in Kültz (2005), who summarized the cellular stress response (CSR) by itemizing the minimal CSR proteome across all eukaryotes. For the remainder of this discussion, we have limited our focus on the changes in proteins we suspect are the most likely protein biomarkers central in mediating cell cycle delay and participating in the CSR.

4.3.1. Signal transduction and regulation of the cell cycle

We have identified 14-3-3 proteins and a number of 14-3-3 homologs (including HS1) with altered expression as a result of UVR treatment. In particular, each of these proteins shifted to a slightly lower molecular weight, which may indicate removal of one or more modulators, including removal of multiple phosphorylations (Fig. 2, Fu et al., 2000). The 14-3-3 proteins are a highly conserved family of proteins that regulate signaling transduction pathways including cell cycle control and apoptosis (Dunaway et al., 2004; Ferl et al., 2002; Fu et al., 2000). The *S. purpuratus* genome encodes three 14-3-3's (Fernandez-Guerra et al., 2006) and among numerous isoforms, phosphorylation modulates the localization and function of 14-3-3 (Fu et al., 2000). Therefore, it is likely that our results indicate changes in the phosphorylation states of at least one isoform of 14-3-3.

The UV-induced cell cycle arrest in mammalian cells is correlated to the concentration or activation (post-translational modification) of cell cycle regulatory proteins (Athar et al., 2000; Gabrielli et al., 1997). Once a cell senses DNA damage, signaling proteins initiate cellular responses, including activation of Checkpoint kinase 1 (Chk1), which utilizes 14-3-3 to deactivate downstream proteins (Dunaway et al., 2004; Liu et al., 2000; Rhind and Russell, 2000). Activated 14-3-3 proteins regulate cell cycle proteins, including Cdc25 and ultimately Cdc2, a component of the mitosis promoting factor (MPF, Dunaway et al., 2004; Giles et al., 2003). Although other cell cycle proteins such as Cdc2, Cdc25 and Chk1 were not identified in our proteomic study, likely because some have pIs outside of the 4–7 pH range, delayed activity of Cdc2 and the presence of Chk1 in *S. purpuratus* have been demonstrated by Adams and Foltz (2002) and Goschke (2005) respectively. Therefore, our identification of the changes in 14-3-3 indicate there may be downstream effects on cell cycle proteins in *S. purpuratus* as has been documented in other organisms (Dunaway et al., 2004; Fu et al., 2000; Giles et al., 2003).

4.3.2. Oxidative stress, metabolism and repair proteins

We identified multiple HSP70 and Cyclophilin D protein spots. These proteins are important for their role as molecular chaperones in both the cytosol and the mitochondria and appear to play roles in the CSR (Kültz, 2005). UV-irradiation of embryos causes the pI of HSP70 to become more acidic, possibly due to post-translational modification and a change in function of HSP70 (Fig. 2A, Leustek et al., 1989). Intriguingly, in a follow up study, we have examined HSP70 using western blotting and found no change in the concentration of HSP70 through early development or due to UVR-irradiation (data not shown). Therefore, the changes we see on 2D gels are likely the result of PTM.

Four isoforms of HSP70 have been studied in the sea urchin *Paracentrotus lividus* (Sconzo et al., 1997). HSP70 localizes on the mitotic asters with Cdc2/Cyclin B in dividing sea urchin oocytes (Geraci et al., 2003) and is required for proper folding of the cytoskeleton (Agueli et al., 2001; Sconzo et al., 1999). HSPs also regulate key cell cycle proteins (Geraci et al., 2003; Helmbrecht et al., 2000). In addition, UV-exposure of cleavage stage sea urchin embryos stimulates HSP70 expression and is an important indicator of UVR stress early in development (Bonaventura et al., 2005, 2006). Taken together, HSP70 is essential to the cell cycle and sea urchin development, plays an important chaperone role in protein folding, and may be refolding damaged proteins, which can ultimately affect the survivorship of sea urchin embryos.

UV-irradiation also affected migration of Cyclophilin D (Fig. 2), a mitochondrial chaperone that protects cells against apoptosis and regulates mitochondrial permeability and is essential for detecting the redox state and recognizing intracellular Ca^{2+} flux (Green and Reed, 1998; Lin and Lechleiter, 2002). Lesser et al. (2003) demonstrated that UVR causes apoptosis of early sea urchin embryos, which was correlated with damage to DNA, production of antioxidant proteins, and increased developmental abnormalities. Therefore, Cyclophilin D may provide some level of protection against apoptosis during stress and may be part of the cellular machinery sensing UV-induced changes in cellular redox states in sea urchin embryos, which are already heightened because of the respiratory burst after fertilization (Shapiro, 1991; Wong et al., 2004).

As part of the CSR, an oxidative burst occurs in stressed cells (Kültz, 2005). We found UV-induced changes in a large number of proteins that are hallmarks of oxidative stress and involved in protecting cells from oxidative damage. For example, proteins involved in redox regulation such as Glutathione peroxidases that reduce ROS and Thioredoxins that reduce thiols, exhibit nearly 4 or 1.5 fold increases in UV-treated embryos, respectively. These results are consistent with recent studies that demonstrate the overall activities of multiple protective anti-oxidative enzymes such as superoxide dismutase, catylase, glutathione peroxidase (GPx) and glutathione reductase (GR) increased due to UVB-exposure of sea urchin embryos (Lesser, 2010; Lesser et al., 2003, Lister et al., 2010). Lister et al. (2010) also demonstrated that both UVA and UVB caused a decrease in reduced glutathione (GSH) content in sea urchin embryos, indicating oxidative damage is occurring and that up-regulation of GR is a response to UV-stress.

Fig. 3. Expression density map for MALDI-TOF MS identified proteins showing significant differences in spot volumes (2-way ANOVA, factors of *S. purpuratus* embryo batch and UVR-treatment, $P<0.03$ based on 2000 permutations). (A) Expression density map for proteins identified within batches of embryos for all treatments at 30 min post-fertilization ($n=6$ for the two UV-treatments), (B) batches of embryos for all treatments at 90 min post-fertilization. Expression density maps highlight two protein clusters showing significant spot expression differences due to UV-treatment on vertical axis. Protein clusters represents differentially expressed protein volumes according to their standardized expression density [note expression density color bar higher (orange), average (black) and lower (blue)]. Hierarchical clustering of each sample is noted on the top of each heat map (UV-protected and UV-treated, numbered by sea urchin embryo batch) using Pearson's Correlation. The spot number and identification is to the right of each row in the expression map.

A

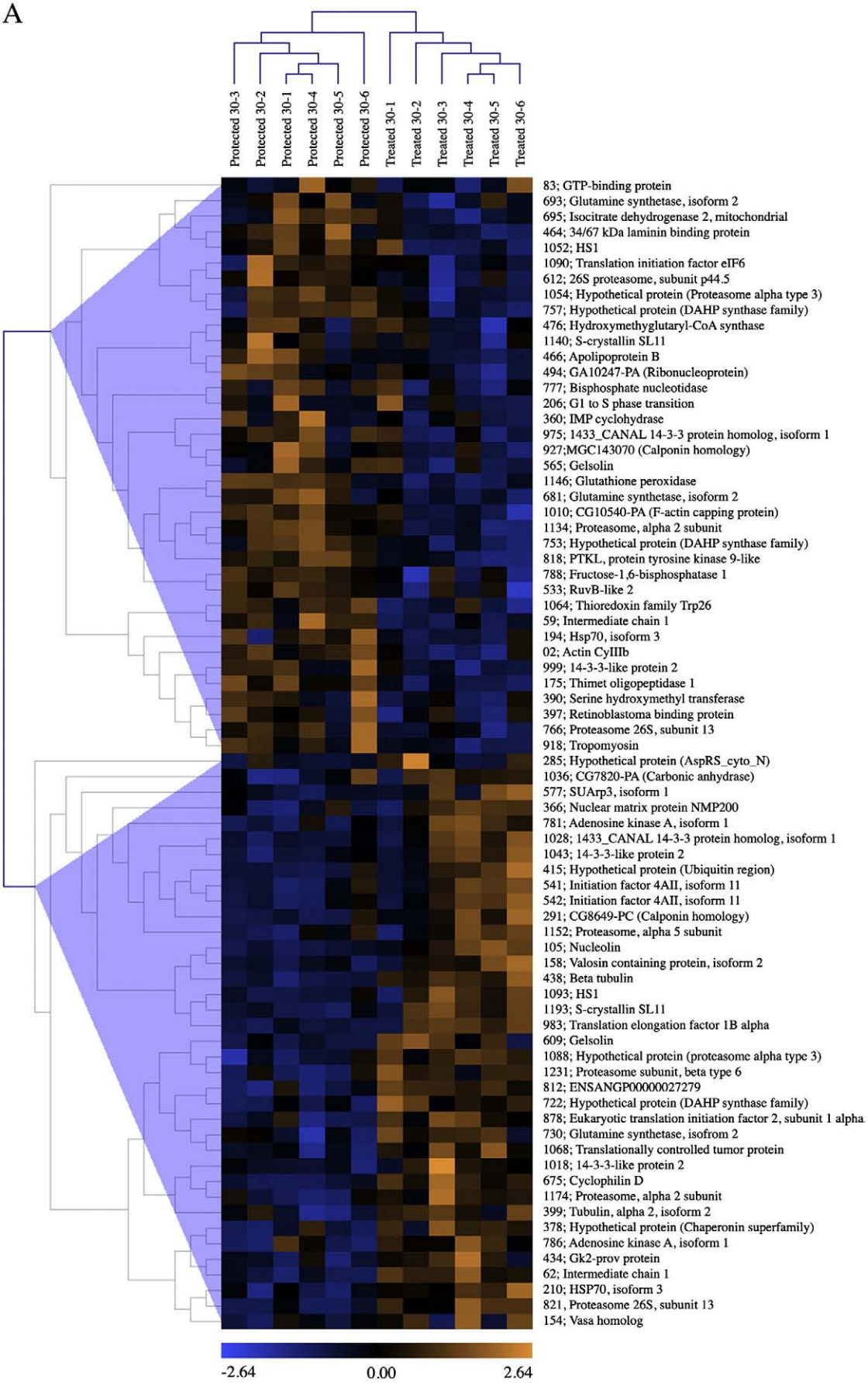
Protected 30-3
Protected 30-2
Protected 30-1
Protected 30-4
Protected 30-5
Protected 30-6
Treated 30-1
Treated 30-2
Treated 30-3
Treated 30-4
Treated 30-5
Treated 30-6
83; GTP-binding protein
693; Glutamine synthetase, isoform 2
695; Isocitrate dehydrogenase 2, mitochondrial
464; 34/67 kDa laminin binding protein
1052; HS1
1090; Translation initiation factor eIF6
612; 26S proteasome, subunit p44.5
1054; Hypothetical protein (Proteasome alpha type 3)
757; Hypothetical protein (DAHP synthase family)
476; Hydroxymethyglutaryl-CoA synthase
1140; S-crystallin SL11
466; Apolipoprotein B
494; GA10247-PA (Ribonucleoprotein)
777; Bisphosphate nucleotidase
206; G1 to S phase transition
360; IMP cyclohydrase
975; 1433_CANAL 14-3-3 protein homolog, isoform 1
927;MGC143070 (Calponin homology)
565; Gelsolin
1146; Glutathione peroxidase
681; Glutamine synthetase, isoform 2
1010; CG10540-PA (F-actin capping protein)
1134; Proteasome, alpha 2 subunit
753; Hypothetical protein (DAHP synthase family)
818; PTKL, protein tyrosine kinase 9-like
788; Fructose-1,6-bisphosphatase 1
533; RuvB-like 2
1064; Thioredoxin family Trp26
59; Intermediate chain 1
194; Hsp70, isoform 3
02; Actin CyIIIb
999; 14-3-3-like protein 2
175; Thimet oligopeptidase 1
390; Serine hydroxymethyl transferase
397; Retinoblastoma binding protein
766; Proteasome 26S, subunit 13
918; Tropomyosin
285; Hypothetical protein (AspRS_cyto_N)
1036; CG7820-PA (Carbonic anhydrase)
577; SUArp3, isoform 1
366; Nuclear matrix protein NMP200
781; Adenosine kinase A, isoform 1
1028; 1433_CANAL 14-3-3 protein homolog, isoform 1
1043; 14-3-3-like protein 2
415; Hypothetical protein (Ubiquitin region)
541; Initiation factor 4AII, isoform 11
542; Initiation factor 4AII, isoform 11
291; CG8649-PC (Calponin homology)
1152; Proteasome, alpha 5 subunit
105; Nucleolin
158; Valosin containing protein, isoform 2
438; Beta tubulin
1093; HS1
1193; S-crystallin SL11
983; Translation elongation factor 1B alpha
609; Gelsolin
1088; Hypothetical protein (proteasome alpha type 3)
1231; Proteasome subunit, beta type 6
812; ENSANGP00000027279
722; Hypothetical protein (DAHP synthase family)
878; Eukaryotic translation initiation factor 2, subunit 1 alpha
730; Glutamine synthetase, isofrom 2
1068; Translationally controlled tumor protein
1018; 14-3-3-like protein 2
675; Cyclophilin D
1174; Proteasome, alpha 2 subunit
399; Tubulin, alpha 2, isoform 2
378; Hypothetical protein (Chaperonin superfamily)
786; Adenosine kinase A, isoform 1
434; Gk2-prov protein
62; Intermediate chain 1
210; HSP70, isoform 3
821, Proteasome 26S, subunit 13
154; Vasa homolog
-2.64
0.00
2.64

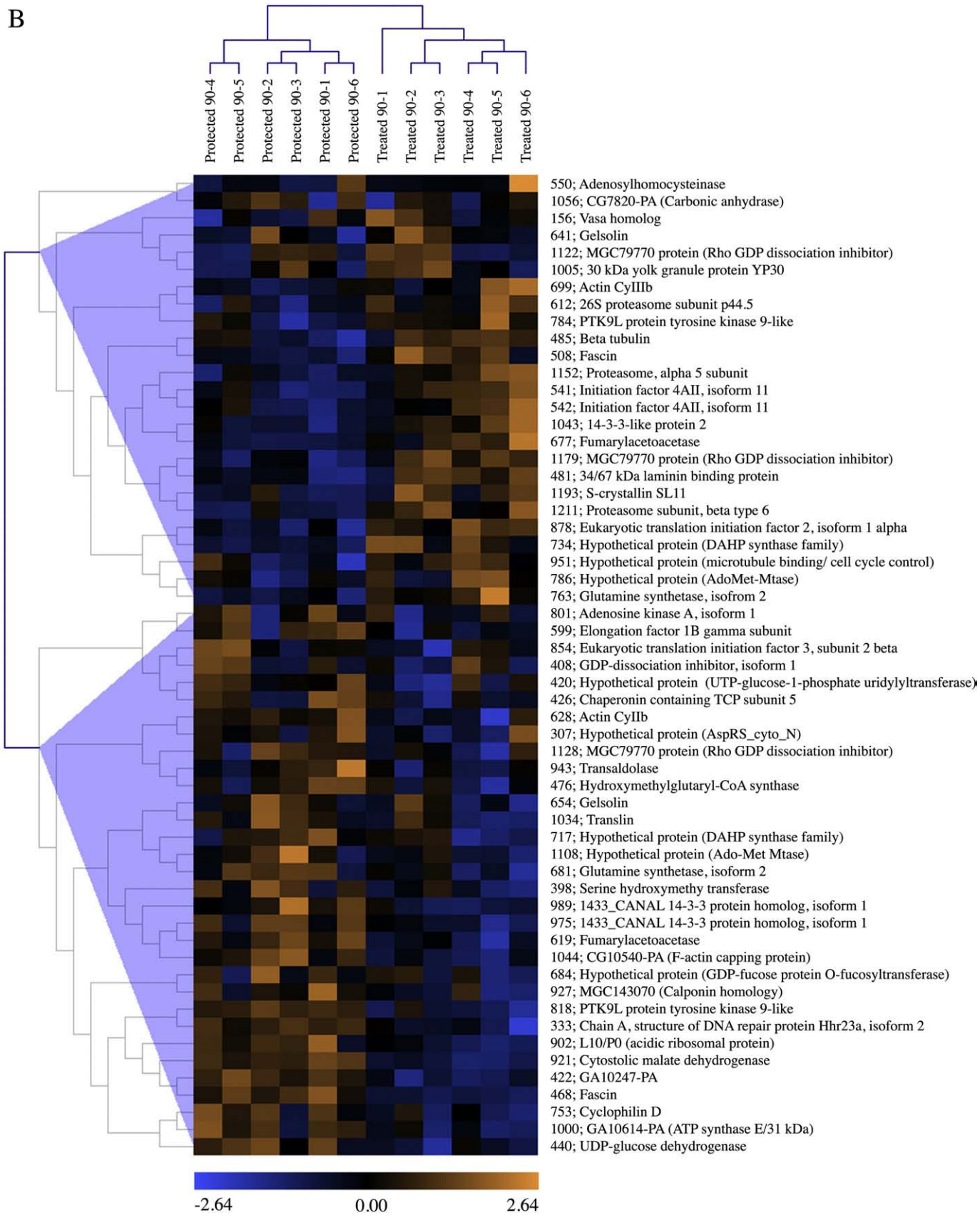

Fig. 3 (*continued*).

Mitochondrial Isocitrate dehydrogenase 2 ($NADP^+$) was down regulated in UV-treated embryos by 1.5 fold at 30 min (Fig. 2, Table 1, Fig. 3). Mitochondrial Isocitrate dehydrogenase functions to recycle $NADP^+$ within the mitochondria and overexpression results in protection from ROS induced damage in mouse NIH3T3 cells (Jo et al., 2001). This protection may be due to the conversion of NADP+ to NAD(P)H, which can produce GSH, facilitating the conversion of hydrogen peroxide to water (see Fig. 11 in Tomanek and Zuzow, 2010). Therefore, our findings suggest UV-irradiated sea urchin embryos may have an altered capacity to cope with additional ROS.

The activity of Isocitrate dehydrogenase is also regulated by glutathionylation during periods of oxidative stress (Kil and Park, 2005), a post-translational modification that could have shifted this protein out of our range of detection or to a spot we were unable to positively identify. Our results, combined with published evidence, may highlight the importance in regulating the activity of this enzyme, especially during UV-induced oxidative stress (Tomanek and Zuzow, 2010). If UV-stressed sea urchin embryos carry a decreased ability to regulate redox flux or use a different strategy to regulate ROS using ovothiols (Epel et al., 1999), the accumulation of damage from ROS could be contributing to macromolecular damage and activation of the CSR.

All of these proteins may function to act simultaneously as the regulators of ROS from the oxidative burst (or metabolism in general) after fertilization and to protect against increased potential for ROS during UVR exposures. These two processes independently are stressful to embryos and may be even more stressful when acting synergistically. Thus, the observed differences in these proteins seem to indicate these embryos may be expending energy to offset damage prior to division. The induction of antioxidant protections in response to UVR and other stressors is likely a common cellular response linking many environmental stressors among all marine organisms (Lesser et al., 2006).

4.3.3. Protein degradation

Many subunits of the major protein-degrading complex, the proteasome (Glickman and Ciechanover, 2002), were differentially regulated by UV-treatment (Fig. 2, Table 1). Our identification of shifts in a large number of proteasome subunits, presumably from PTM, highlights the probable importance of the entire proteasome complex in regulating transitional phases of the cell cycle responding to UVR. In general, PTM's regulate the proteasomal activity (Sumegi, et al., 2003; Zhang et al., 2003, 2007) and inhibition of the proteasome blocks mitosis in sea urchin embryos by delaying the activation of MPF (dephosphorylation of Cdc2) and regulating the exit from S-phase (Kawahara et al., 2000).

In our experiments, UV-irradiation caused changes in expression levels of several proteins known to interact and modify proteasome activity and the cell cycle including Hsp70, Hhr23 and p53 (Verma et al., 2000; Glockzin et al., 2003). The 26S proteasome subunit stabilizes nucleotide excision repair (NER) using Hhr23, providing yet another potential link between the detection of DNA damage and the control of the cell cycle regulated through the proteasome (Glockzin et al., 2003). UV-stress, causes the entire proteasome complex to mediate the polyubiquination and subsequent degradation of p53 (Glockzin et al., 2003; Kültz, 2005). Although apoptosis during sea urchin embryogenesis is rare, sea urchin embryos can undergo a change in the frequency of apoptosis during stress (Vega Thurber and Epel, 2007). Moreover, UV-induced DNA damage can cause imbalances in p53 and p21 expression, leading to the activation of apoptotic pathways during sea urchin development (Lesser et al., 2003). Similarly, Tomanek and Zuzow (2010) have proposed a balance of protein degradation by ubiquitin-conjugation and ATP consumption, which may be linked to heat stress. Overall, these studies indicate that the balance of proteasomal function may be shifted during UV-stress and suggest it is a general response to stress that may be shared among marine organisms.

4.3.4. Cytoskeleton and cytoskeleton regulating proteins

We identified differential spot migration of numerous cytoskeletal proteins including actins and tubulins from all time points and UV-treatments (Table 1). Presumably their regulation is by a PTM resulting from differences in cytoskeletal assembly because we do not typically see differences in the total amount of these proteins due to UVR (Campanale, personal observation) or during early development (Roux et al., 2008). Also, we believe the regulation of these proteins is part of UV-induced cell cycle delay because we tracked Gelsolin (Fig. 2, Table 1, Fig. 3), a regulator of actin polymerization/severing (Sun et al., 1999), in all treatments and all time points. The change in migration of Gelsolin is particularly interesting because it may indicate that UV-treated embryos are physically stalled in the cell cycle due to actin cytoskeleton dysfunction. Further, we document a 1.4 fold increase in SUArp3, an actin-related protein, and a 1.3 fold decrease in F-actin capping protein indicating that regulation of the cytoskeleton is altered after UV-treatment and may be associated with UV-induced cell cycle delays (Rustad, 1971).

We were also able to track multiple protein spots identified as Rho-GDP dissociation inhibitor at 90 min (Table 1, spots 1122, 1128 and 1179 in Figs. 2A, 3A). Rho-GTPases appear to play a role in cytokinesis by promoting the assembly of microtubules especially during interphase of the cell cycle (Robinson and Spudich, 2000). Our identification of the differential migration of Rho family inhibiting proteins may specify coordinated signaling within these cells, ultimately preventing the assembly of the cytoskeleton during developmental delay.

Differences in regulation of cytoskeleton proteins are logical because UV-induced delays in cell division are linked to the activities of the proteins controlling the physical aspects of pronuclear localization, chromosomal segregation, cleavage furrow formation and the actual separation of daughter cells. Ultimately, MPF is important in regulating cytoskeletal elements via phosphorylation (Robinson and Spudich, 2000) and therefore, MPF-regulators such as HSP70 and 14-3-3, discussed above, may also be important regulators of the cytoskeleton. Very little attention has been given to effects of UVR on cytoskeletal elements, but importantly, UVR disrupts cytoplasmic microtubules in human skin cells (Zamansky and Chou, 1987) and affects microtubule stability (Veselská and Janisch, 2000).

4.3.5. Protein translation

Iordanov et al. (1998) has asserted, responses to UV-stress may be generated at the ribosome from damaged rRNA. We identified L10e/P0 (an acidic ribosomal protein) as decreasing nearly 1.3 fold in UV-treated cells. Further, we have identified increases in proteins spots for eIF2α and eIF4AII, proteins required for the initiation of translation in all UV-treated embryos. eIF2α kinases play a role in UV-induced apoptosis in human cells, in part due to the phosphorylation of eIF2α (Parker et al., 2006). Last, we identified a two-fold increase in Nucleolin in the UV-treated lysates. Overexpression of Nucleolin inhibits the translation of p53 and the loss of Nucleolin promotes the expression of p53 along with ribosomal subunits after DNA damage (Takagi et al., 2005). Although we cannot state if the protein spot we identified is the active or inactive form of Nucleolin, its function may be controlled by Cdc2 mediated phosphorylation (Belenguer et al., 1990) and may have a role in stalling the cell cycle by altering the levels of p53 during and after UV-exposure (Pavey et al., 2001). The identification of Nucleolin coupled with evidence of its function and the UV-induced induction of p53 (Lesser et al., 2003) suggests there is a delicate balance between ROS, cell cycle and the regulation of apoptosis.

5. Conclusions

In conclusion, we provide the most comprehensive documentation of the proteome responses in the sea urchin early cleavage stage embryos to UV-stress to date. The list of proteins we identified are representatives from many different cellular pathways affected by UVR including cell cycle, protein turnover and stress regulation, and are potential protein candidates for future functional studies. A subset of the proteins identified here may help resolve the longstanding questions regarding the mechanism by which UV-stress alters cellular physiology, cell cycle delay and developmental abnormalities. Also, detection of specific PTMs of the proteins we identified is essential to understanding both their regulation and activity during UV-stress. A major challenge in the coming years will be to characterize these pathways and proteins in an effort to better understand the mechanisms involved in UV-stress controlling cellular physiology. Assessing UV-stress physiology will elucidate the impact future fluctuations in UVR will have on marine invertebrate embryos specifically and cells in general. Understanding the response of the entire *S. purpuratus* proteome to UVR-exposure will eventually provide insights into the future potential effects of climate change, including the synergistic effects of UVR and other physical factors, at the molecular level.

Acknowledgements

We would like to especially thank Dr. Kathy Foltz for her expert advice, generous training and guidance improving this manuscript. We also thank Dr. Michelle Roux for her patience and help with running 2DGE. A special thank you goes to Shane Anderson and Christoph Pierre at The University of California at Santa Barbara who collected the sea urchins used in this work. In addition, we thank Tom Moylan and Jason Felton for helping us maintain these sea urchins at the Cal Poly Center for Coastal Marine Sciences. We also appreciate valuable feedback we received from Dr. Amro Hamdoun, Dr. Victor Vacquier. This research was supported through a CSUPERB Faculty Seed Grant and through NSF Grant IBN 0417003 awarded to N. L. Adams. **[SS]**

References

Adams, N.L., Foltz, K.R., 2002. A molecular approach to understanding UV-induced mitotic delay in sea urchin embryos. Proceedings from the North American Echinoderm Conference 2001. Gulf of Mexico Sciences 19, 165.

Adams, N.L., Shick, J.M., 1996. Mycosporine-like amino acids provide protection against ultraviolet radiation in eggs of the green sea urchin *Strongylocentrotus droebachiensis*. Photochem. Photobiol. 64, 149–158.

Adams, N.L., Shick, J.M., 2001. Mycosporine-like amino acids prevent UVB-induced abnormalities during early development of the green sea urchin *Strongylocentrotus droebachiensis*. Mar. Biol. 138, 267–280.

Adams, N., Shick, J.M., Dunlap, W., 2001. Selective accumulation of mycosporine-like amino acids in ovaries of green sea urchin, *Strongylocentrotus droebachiensis*, is not affected by ultraviolet radiation. Mar. Biol. 138, 284–294.

Agueli, C., Geraci, F., Giudice, G., Chimenti, L., Cascino, D., Sconzo, G., 2001. A constitutive 70 kDa heat-shock protein is localized on the fibers of spindles and asters at metaphase in an ATP-dependent manner: a new chaperone role is proposed. Biochem. J. 360, 413–419.

Anderson, S., Hoffman, J., Wild, G., Bosch, I., Karentz, D., 1993. Cytogenetic, cellular, and developmental responses in Antarctic sea urchins (*Starchiness neumayeri*) following laboratory ultraviolet-B and ambient solar radiation exposures. Antarct. J. 28, 115–116.

Anderson, S., Zepp, R., Machula, J., Santavy, D., Hansen, L., Mueller, E., 2001. Indicators of UV exposure in corals and their relevance to global climate change and coral bleaching. Hum. Ecol. Risk Assess. 7, 1271–1282.

Athar, M., Kim, A.L., Ahmad, N., Mukhtar, H., Gautier, J., Bickers, D.R., 2000. Mechanism of ultraviolet B-induced cell cycle arrest in G2/M phase in immortalized skin keratinocytes with defective p53. Biochem. Bioph. Res. Co. 277, 107–111.

Bancroft, B.A., Baker, N.J., Blaustein, A.R., 2007. Effects of UVB on marine and freshwater organisms: a synthesis through meta-analysis. Ecol. Lett. 10, 332–345.

Belenguer, P., Caizergues-Ferrer, M., Labbé, J.C., Dorée, M., Amalric, F., 1990. Mitosis-specific phosphorylation of nucleolin by p34cdc2 protein kinase. Mol. Cell. Biol. 10, 3607–3618.

Berth, M., Moser, F.M., Kolbe, M., Bernhardt, J., 2007. The state of the art in the analysis of two dimensional gel electrophoresis images. Appl. Microbiol. Biotechnol. 76, 1223–1243.

Bonaventura, R., Poma, V., Costa, C., Matranga, V., 2005. UVB radiation prevents skeleton growth and stimulates expression of stress markers in sea urchin embryos. Biochem. Bioph. Res. Co. 328, 150–157.

Bonaventura, R., Poma, V., Russo, R., Zito, F., Matranga, V., 2006. Effects of UV-B radiation on development and hsp70 expression in sea urchin cleavage embryos. Mar. Biol. 149, 79–86.

Bradham, C.A., Foltz, K.R., Beane, W.S., Arnone, M.I., Rizzo, F., Coffman, J.A., Mushegan, A., Goel, M., Morales, J., Geneviere, A., Laparz, F., Robertson, A.J., Kelkar, H., Loza-Coll, M., Townley, I.K., Raish, M., Roux, M.M., Lepage, T., Gache, C., McClay, D.R., Manning, G., 2006. The sea urchin kinome: a first look. Dev. Biol. 300, 180–193.

Caldwell, M.M., Björn, L.O., Bornman, J.F., Kulandiavelu, G., Teramura, A.H., Tevini, M., 1998. Effects of increased solar ultraviolet radiation on terrestrial ecosystems. J. Photoch. Photobio. B. 46, 40–52.

Cullen, J., Neale, P., 1994. Ultraviolet radiation, ozone depletion, and marine photosynthesis. Photosynth. Res. 39, 303–320.

Dunaway, S., Liu, H., Walworth, N., 2004. Interaction of 14-3-3 protein with Chk1 affects localization and checkpoint function. Journal of Cell Science. 118, 39–50.

Epel, D., Hemela, K., Shick, M., Patton, C., 1999. Development in the floating world: defenses of eggs and embryos against damage from UV-radiation. Am. Zool. 39, 271–278.

Ferl, R.J., Manak, M.S., Reyes, M.F., 2002. The 14-3-3s. Genome Biol. 3, 3010.1–3010.7.

Fernandez-Guerra, A., Aze, A., Morales, J., Mulner-Lorillon, O., Cosson, B., Cormier, P., Bradham, C., Adams, N.L., Robertson, A.J., Marzluff, W.F., Coffman, J.A., Genevière, A.M., 2006. The genomic repertoire for cell cycle control and DNA metabolism in *S. purpuratus*. Dev. Biol. 300, 238–251.

Fu, H., Subramanian, R.R., Masters, S.C., 2000. 14-3-3 Proteins: structure, function, and regulation. Annu. Rev. Pharmacol. 40, 617–647.

Gabrielli, B.G., Clark, J.M., McCormack, A.K., Ellem, K.A.O., 1997. Ultraviolet light-induced G2 phase cell cycle checkpoint blocks cdc25-dependent progression into mitosis. Oncogene. 15, 749–758.

Geraci, F., Agueli, C., Giudice, G., Sconzo, G., 2003. Localization of HSP70, Cdc2, and cyclin B in sea urchin oocytes in non-stressed conditions. Biochem. Bioph. Res. Co. 310, 748–753.

Giese, A., 1964. Studies on ultraviolet radiation action upon animal cells. In: Giese, A. (Ed.), Photophysiology, vol II. Academic, New York, pp. 203–245.

Giles, N., Forrest, A., Gabrielli, B., 2003. 14-3-3 acts as an intramolecular bridge to regulate cdc25B localization and activity. J. Biol. Chem. 278, 28580–28587.

Glickman, M.H., Ciechanover, A., 2002. The ubiquitin–proteasome proteolytic pathway: destruction for the sake of construction. Physiol. Rev. 82, 373–428.

Glockzin, S., Ogi, F.X., Hengstermann, A., Scheffner, M., Blattner, C., 2003. Involvement of the DNA repair protein hHR23 in p53 degradation. Mol. Cell Biol. 23, 8960–8969.

Goel, M., Mushegian, A., 2006. Intermediary metabolism in sea urchin: the first inferences from the genome sequence. Dev. Biol. 300, 282–292.

Goldstone, J.V., Hamdoun, A., Cole, B.J., Howard-Ashby, M., Nebert, D.W., Scally, M., Dean, M., Epel, D., Hahn, M.E., Stegean, J.J., 2006. The chemical defensome: environmental sensing and response genes in the *Strongylocentrotus purpuratus* genome. Dev. Biol. 300, 366–384.

Goschke, G.A., 2005. The presence and activity of Chk1 in the UV-induced cellular response in the purple sea urchin, *Strongylocentrotus purpuratus.* M.S. Thesis, California Polytechnic State University, San Luis Obispo.

Green, D.R., Reed, J.C., 1998. Mitochondria and apoptosis. Science 281, 1309–1312.

Häder, D., Kumar, H., Smith, R., Worrest, R., 2007. Effects of solar UV radiation on aquatic ecosystems and interactions with climate change. Photochem. Photobiol. Sci. 6, 267–285.

Hamdoun, A., Epel, D., 2007. Embryo stability and vulnerability in an always changing world. Proc. Natl. Acad. Sci. 104, 1745–1750.

Hamer, B., Pavičić Hamer, D., Müller, W.E.G., Batel, R., 2004. Stress-70 proteins in marine mussel *Mytilus galloprovincialis* as biomarkers of environmental pollution: a field study. Environ. Int. 30, 873–882.

Helmbrecht, K., Zeise, E., Rensing, L., 2000. Chaperones in cell cycle regulation and mitogenic signal transduction: a review. Cell Prolif. 33, 341–365.

Hoegh-Guldberg, O., Hughes, L., McIntyre, S., Lindenmayer, D.B., Pamesan, C., Possingham, H.P., Thomas, C.D., 2008. Assisted colonization and rapid climate change. Science. 321, 345–346.

Hollósy, F., 2002. Effects of ultraviolet radiation on plant cells. Micron. 33, 179–197.

Howard-Ashby, M., Materna, S.C., Brown, T., Tu, Q., Oliveri, P., Cameron, R.A., Davidson, E.H., 2006. High regulatory gene use in sea urchin embryogenesis: implications for bliaterian development and evolution. Dev. Biol. 300, 27–34.

Imlay, J., Linn, S., 1988. DNA damage and oxygen radical toxicity. Science. 240, 1302–1309.

Iordanov, M.S., Pribnow, D., Magun, J.L., Dinh, T.H., Pearson, J.A., Magun, B.E., 1998. Ultraviolet radiation triggers the ribotoxic stress response in mammalian cells. J. Biol. Chem. 273, 15794–15803.

Isley, N.M., Lamare, C. Marchall, Barker, M., 2009. Expression of the DNA repair enzyme, Photolyase, in developmental tissues and larvae, and in response to ambient UV-R in the Antarctic sea urchin Sterchinuc neumayeri. Photochem. Photobiol. 85, 1168–1172.

Jackson, G.A., Strathmann, R.R., 1981. Larval mortality from offshore mixing as a link between precompetent and competent periods of development. Am. Nat. 118, 16–26.

Jo, S.H., Son, M.K., Koh, H.J., Lee, S.M., Song, I.H., Kim, Y.O., Lee, Y.S., Jeong, K.S., Kim, W.B., Park, J.W., Song, B.J., Huhe, T.L., 2001. Control of mitochondrial redox balance and cellular defense against oxidative damage by mitochondrial NADP+-dependent isocitrate dehydrogenase. J. Biol. Chem. 276, 16168–16176.

Kawahara, H., Phillipova, R., Yokosawa, H., Patel, R., Tanaka, K., Whitaker, M., 2000. Inhibiting proteasome activity causes overreplication of DNA and blocks entry into mitosis in sea urchin embryos. J Cell Sci. 113, 2659–2670.
Kerr, J., McElroy, C., 1993. Evidence for large upward trends of ultraviolet radiation linked to ozone depletion. Science. 262, 1032–1034.
Kil, I.S., Park, J.W., 2005. Regulation of mitochondrial NADP+-dependent isocitrate dehydrogenase activity by glutathionylation. J. Biol. Chem. 280, 10846–10854.
Kültz, D., 2005. Molecular and evolutionary basis of the cellular stress response. Annu. Rev. Physiol. 67, 225–257.
Lamare, M.D., Hoffman, J., 2004. Natural variation of carotenoids in the eggs and gonads of the echinoid genus, *Strongylocentrotus*: implications for their role in ultraviolet radiation photoprotection. J. Exp. Mar. Biol. Ecol. 312, 215–233.
Lamare, M.D., Barker, M.F., Lesser, M.P., Marshall, C.J., 2006. DNA photorepair in echinoid embryos: effects of temperature on repair rate in Antarctic and non-Antarctic species. J. Exp. Biol. 209, 5017–5028.
Lamare, M.D., Barker, M.F., Lesser, M.P., 2007. In situ rates of DNA damage and abnormal development in Antarctic and non-Antarctic sea urchin embryos. Aquatic Biology 1, 21–32.
Lesser, M.P., 2010. Depth-dependent effects of ultraviolet radiation on survivorship, oxidative stress and DNA damage in sea urchin (*Strongylocentrotus droebachiensis*) embryos from the Gulf of Maine. Photochem Photobiol. 8, 382–388.
Lesser, M., Kruse, V., Barry, T., 2003. Exposure to ultraviolet radiation causes apoptosis in developing sea urchin embryos. J. Exp. Biol. 206, 4097–4103.
Lesser, M.P., Barry, T.M., Lamare, M.D., Barker, M.F., 2006. Biological weighting functions for DNA damage in sea urchin embryos exposed to ultraviolet radiation. J. Exp. Mar. Biol. Ecol. 328, 10–21.
Leustek, T., Dalie, B., Amir-Shapira, D., Brot, N., Weissbach, H., 1989. A member of the Hsp70 family is localized in mitochondria and resembles *Escherichia coli* DnaK. Proc. Natl. Acad. Sci. 86, 7805–7808.
Lin, D., Lechleiter, J.D., 2002. Mitochondrial targeted cyclophilin D protects cells from cell death by peptidyl prolyl isomerization. J. Biol. Chem. 277, 31134–31141.
Lister, K.N., Lamare, M.D., Burritt, D.J., 2010. Oxidative damage in response to natural levels of UV-B radiation in larvae of the tropical sea urchin *Tripneustes gratilla*. Photochem. Photobio. 86, 1091–1098.
Liu, Q., Guntuku, S., Cui, X., Matsuoka, S., Cortez, D., et al., 2000. Chk1 is an essential kinase that is regulated by Atr and required for the G2/M DNA damage checkpoint. Genes and Development. 14, 1448–1459.
Livingston, B.T., Killian, C.E., Wilt, F., Cameron, A., Landrum, M.J., Ermolaeva, O., Sapojnikov, V., Maglott, D.R., Buchanan, A.M., Ettensohn, C.A., 2006. A genome-wide analysis of biomineralization-related proteins in the sea urchin *Strongylocentrotus purpuratus*. Dev. Biol. 300, 335–348.
Madronich, S., Mckenzie, R., Bjorn, L., Caldwell, M., 1998. Changes in biologically active ultraviolet radiation reaching the Earth's surface. In: van der Leun, J., Tang, X., Tevini, M. (Eds.), Environmental Effects of Ozone Depletion: 1998 Assessment. United Nations, New York, pp. 5–19. Environment programme report.
Marchler-Bauer, A., Anderson, J.B., Chitsaz, F., Derbyshire, M.K., DeWeese-Scott, C., Fong, J.H., Geer, L.Y., Geer, R.C., Gonzales, N.R., Gwadz, M., He, S., Hurwitz, D.I., Jackson, J.D., Ke, Z., Lanczycki, C.J., Leibert, C.A., Liu, C., Lu, F., Lu, S., Marchler, G.H., Mullokandov, M., Song, J.S., Tasneem, A., Thanki, N., Yamashita, R.A., Zhang, D., Zhang, N., Bryant, S.H., 2009. CDD: specific functional annotation with the conserved domain database. Nucleic Acids Res. 37, D205–D210.
McKenzie, R., Bijorn, L., Bais, A., Ilyasd, M., 2003. Changes in biologically active ultraviolet radiation reaching the Earth's surface. Photochem. Photobiol. Sci. 2, 5–15.
McKenzie, R.L., Aucamp, P.J., Bais, A.F., Björn, L.O., Ilyasd, M., 2007. Changes in biologically-active ultraviolet radiation reaching the Earth's surface. Photochem. Photobiol. Sci. 6, 218–231.
Morgan, S.G., Christy, J.H., 1996. Survival of marine larvae under the countervailing selective pressures of photodamage and predation. Limnol. Oceanogr. 41, 498–504.
Parker, S.H., Parker, T.A., George, K.S., Wu, S., 2006. The roles of translation initiation regulation in ultraviolet light-induced apoptosis. Mol. Cell Biochem. 293, 173–181.
Pavey, S., Russell, T., Gabrielli, B., 2001. G2 phase cell cycle arrest in human skin following UV irradiation. Oncogene. 20, 6103–6110.
Peak, M., Peak, J., 1990. Hydroxyl radical quenching agents protect against DNA breakage caused by both 365-nm and gamma radiation. Photochem. Photobiol. 51, 649–652.
Pechenik, J.A., 1987. Environmental influences on larval survival and development. In: Giese, A. C., Pearse, J. S., Pearse, V. B. (eds.) Reproduction of marine invertebrates, Vol. IX. Blackwell Scientific Publications and Boxwood Press, Cambridge, 511-608.
Perkins, D.N., Pappin, D.J.C., Creasy, D.M., Cottrell, J.S., 1999. Probability-based protein identification by searching sequence databases using mass spectrometry data. Electrophoresis. 20, 3551–3567.
Pesando, D., Huitorel, P., Dolcini, V., Angelini, C., Guidetti, P., Falugi, C., 2003. Biological targets of neurotoxic pesticides analyzed by alteration of developmental events in the Mediterranean sea urchin, *Paracentrotus lividus*. Mar. Environ. Res. 55, 39–57.
Pourzand, C., Tyrell, R.M., 1999. Apoptosis, the role of oxidative stress and the example of solar UV radiation. Photochem. Photobiol. 70, 380–390.
Przeslawski, R., 2005. Combined effects of solar radiation and desiccation on the mortality and development of encapsulated embryos of rocky shore gastropods. Mar. Ecol. Prog. Ser. 298, 169–177.
Rao, B., Hindgardner, R., 1965. Analysis of DNA synthesis and x-ray-induced mitotic delay in sea urchins. Radiat. Res. 26, 534–537.
Rhind, N., Russell, P., 2000. Chk1 and Cds1: linchpins of the DNA damage and replication checkpoint pathways. Journal of Cell Science. 113, 3889–3896.
Robinson, D.N., Spudich, J.A., 2000. Towards a molecular understanding of cytokinesis. Trends Cell Biol. 10, 228–237.
Roux, M.M., Radeke, M., Goel, M., Mushegian, A., Foltz, K.R., 2008. 2DE identification of proteins exhibiting turnover and phosphorylation dynamics during sea urchin egg activation. Dev. Biol. 313, 630–647.
Russo, R., Bonaventura, R., Zito, F., Schroder, H., Muller, I., Muller, W., Matranga, V., 2003. Stress to cadmium monitored by metallothionein gene induction in *Paracentrotus lividus* embryos. Cell Stress Chaperon. 8, 232–241.
Rustad, R., 1960. Changes in the sensitivity to ultraviolet-induced mitotic delay during the cell division cycle of the sea urchin egg. Exp. Cell Res. 21, 596–602.
Rustad, R., 1971. Radiation responses during the mitotic cycle of the sea urchin egg. In: Cameron, I., Padilla, G., Zimmerman, A. (Eds.), Developmental aspects of the cell cycle. Academic, New York, pp. 127–159.
Saeed, A.I., Sharov, V., White, J., Li, J., Liang, W., Bhagabati, N., Braisted, J., Klapa, M., Currier, T., Thiagarajan, M., Sturn, A., Snuffin, M., Rezantsev, A., Popov, D., Ryltsov, A., Kostukovich, E., Borisovsky, I., Liu, Z., Vinsavich, A., Trush, V., Quackenbush, J., 2003. TM4: a free, open-source system for microarray data management and analysis. Biotechniques. 34, 374–378.
Samanta, M.P., Tongprasit, W., Istrail, S., Cameron, R.A., Tu, Q., Davidson, E.H., Stolc, V., 2006. The transcriptome of the sea urchin embryo. Science. 314, 960–962.
Sconzo, G., Amore, G., Capra, G., Giudice, G., Cascino, D., Ghersi, G., 1997. Identification and characterization of a constitutive HSP75 in sea urchin embryos. Biochem. Bioph. Res. Co. 234, 24–29.
Sconzo, G., Palla, F., Agueli, C., Spinelli, G., Giudice, G., Cascino, D., Geraci, F., 1999. Constitutive hsp70 is essential to mitosis during early cleavage of *Paracentrotus lividus* embryos: the blockage of constitutive hsp70 impairs mitosis. Biochem. Bioph. Res. Co. 260, 143–149.
Setlow, R., 1974. The wavelengths in sunlight effective in producing skin cancer. A theoretical analysis. Proc. Natl. Acad. Sci. USA 71, 3363–3366.
Shapiro, B.M., 1991. The control of oxidant stress at fertilization. Science. 252, 533–536.
Shick, J.M., Romaine-Loud, S., Ferrier-Pages, C., Gattuso, J.-P., 1999. Ultraviolet-B radiation stimulates shikimate pathway-dependent accumulation of mycosporine-like amino acids in the coral *Stylophora pistillata* despite decreases in its population of symbiotic dinoflagellates. Limnol. Oceanogr. 44, 1667–1682.
Smith, R.C., Baker, K.S., 1979. Penetration of UV-B and biologically effective dose-rates in natural waters. Photochem. Photobio. 29, 311–323.
Smith, R., Prezlin, B., Baker, K., Bidigare, R., Boucher, N., Coley, T., Karentz, D., MacIntyre, S., Matlick, H., Menzies, D., Ondrusek, M., Wan, Z., Water, K., 1992. Ozone depletion: ultraviolet radiation and phytoplankton biology in natural waters. Science. 255, 252–259.
Sodergren, E., Weinstock, G.M., Davidson, E.H., Cameron, R.A., Gibbs, R.A., Angerer, R.C., Angerer, L.M., Arnone, M.I., Burgess, D.R., Burke, R.D., Coffman, J.A., Dean, M., Elphick, M.R., Ettensohn, C.A., Foltz, K.R., Hamdoun, A., Hynes, R.O., Klein, W.H., Marzluff, W., McClay, D.R., Morris, R.L., Mushegian, A., Rast, J.P., Smith, L.C., Thorndyke, M.C., Vacquier, V.D., Wessel, G.M., Wray, G., Zhang, L., Elsik, C.G., Ermolaeva, O., Hlavina, W., Hofmann, G., Kitts, P., Landrum, M.J., Mackey, A.J., Maglott, D., Panopoulou, G., Poustka, A.J., Pruitt, K., Sapojnikov, V., Song, X., Souvorov, A., Solovyev, V., Wei, Z., Whittaker, C.A., Worley, K., Durbin, K.J., Shen, Y., Fedrigo, O., Garfield, D., Haygood, R., Primus, A., Satija, R., Severson, T., Gonzalez-Garay, M.L., Jackson, A.R., Milosavljevic, A., Tong, M., Killian, C.E., Livingston, B.T., Wilt, F.H., Adams, N., Belle, R., Carbonneau, S., Cheung, R., Cormier, P., Cosson, B., Croce, J., Fernandez-Guerra, A., Geneviere, A.M., Goel, M., Kelkar, H., Morales, J., Mulner-Lorillon, O., Robertson, A.J., Goldstone, J.V., Cole, B., Epel, D., Gold, B., Hahn, M.E., Howard-Ashby, M., Scally, M., Stegeman, J.J., Allgood, E.L., Cool, J., Judkins, K.M., McCafferty, S.S., Musante, A.M., Obar, R.A., Rawson, A.P., Rossetti, B.J., Gibbons, I.R., Hoffman, M.P., Leone, A., Istrail, S., Materna, S.C., Samanta, M.P., Stolc, V., Tongprasit, W., Tu, Q., Bergeron, K.F., Brandhorst, B.P., Whittle, J., Berney, K., Bottjer, D.J., Calestani, C., Peterson, K., Chow, E., Yuan, Q.A., Elhaik, E., Graur, D., Reese, J.T., Bosdet, I., Heesun, S., Marra, M.A., Schein, J., Anderson, M.K., Brockton, V., Buckley, K.M., Cohen, A.H., Fugmann, S.D., Hibino, T., Loza-Coll, M., Majeske, A.J., Messier, C., Nair, S.V., Pancer, Z., Terwilliger, D.P., Agca, C., Arboleda, E., Chen, N., Churcher, A.M., Hallbook, F., Humphrey, G.W., Idris, M.M., Kiyama, T., Liang, S., Mellott, D., Mu, X., Murray, G., Olinski, R.P., Raible, F., Rowe, M., Taylor, J.S., Tessmar-Raible, K., Wang, D., Wilson, K.H., Yaguchi, S., Gaasterland, T., Galindo, B.E., Gunaratne, H.J., Juliano, C., Kinukawa, M., Moy, G.W., Neill, A.T., Nomura, M., Raisch, M., Reade, A., Roux, M.M., Song, J.L., Su, Y.H., Townley, I.K., Voronina, E., Wong, J.L., Amore, G., Branno, M., Brown, E.R., Cavalieri, V., Duboc, V., Duloquin, L., Flytzanis, C., Gache, C., Lapraz, F., Lepage, T., Locascio, A., Martinez, P., Matassi, G., Matranga, V., Range, R., Rizzo, F., Rottinger, E., Beane, W., Bradham, C., Byrum, C., Glenn, T., Hussain, S., Manning, G., Miranda, E., Thomason, R., Walton, K., Wikramanayke, A., Wu, S.Y., Xu, R., Brown, C.T., Chen, L., Gray, R.F., Lee, P.Y., Nam, J., Oliveri, P., Smith, J., Muzny, D., Bell, S., Chacko, J., Cree, A., Curry, S., Davis, C., Dinh, H., Dugan-Rocha, S., Fowler, J., Gill, R., Hamilton, C., Hernandez, J., Hines, S., Hume, J., Jackson, L., Jolivet, A., Kovar, C., Lee, S., Lewis, L., Miner, G., Morgan, M., Nazareth, L.V., Okwuonu, G., Parker, D., Pu, L.L., Thorn, R., Wright, R., 2006. The genome of the sea urchin *Strongylocentrotus purpuratus*. Science 314, 941–952.
Stitzel, M.L., Seydoux, G., 2007. Regulation of the oocyte-to-zygote transition. Science. 316, 407–408.
Strathmann, R.R., Staver, J.M., Hoffman, J.R., 2002. Risk and the evolution of cell-cycle durations of embryos. Evolution. 56, 708–720.
Sumegi, M., Hunyadi-Gulyas, E., Medzihradszky, K.F., Udvardy, A., 2003. 26S proteasome subunits are *O*-linked *N*-acetylglucosamine-modified in *Drosophila melanogaster*. Biochem. Biophys. Res. Commun. 312, 1284–1289.
Sun, H.Q., Yamamoto, M., Mejullano, M., Yin, H.L., 1999. Gelsolin, a multifunctional actin regulatory protein. J. Biol. Chem. 274, 33179–33182.
Takagi, M., Absalon, M.J., McLure, K.G., Kastan, M.B., 2005. Regulation of p53 translation and induction after DNA damage by ribosomal protein and nucleolin. Cell. 123, 49–63.
Tatusov, R.L., Fedorova, N.D., Jackson, J.D., Jacobs, A.R., Kiryutin, B., Koonin, E.V., Krylov, D.M., Mazumder, R., Mekhedov, S.L., Nikolskaya, A.N., Rao, B.S., Smirnov, S., Sverdlov,

A.V., Vasudevan, S., Wolf, Y.I., Yin, J.J., Natale, D.A., 2003. The COG database: and updated version includes eukaryotes. BMC. Bioinfo. 4, 41.
Tedetti, M., Sempere, R., 2006. Percentage of ultraviolet radiation in the marine environment. A review. Photochem. Photobiol. 82, 389–397.
Tevini, M., 1993. Molecular biological effects of ultraviolet radiation. In: Tevini, M. (Ed.), UV-B Radiation and Ozone Depletion: Effects on Humans, Animals, Plants, Microorganisms, and Materials. Lewis Publishers, Baca Raton, FL, pp. 1–16.
Tomanek, L., 2005. Two-dimensional gel analysis of the heat-shock response in marine snails (genus *Tegula*): interspecific variation in protein expression and acclimation ability. J. Exp. Biol. 208, 3133–3143.
Tomanek, L., 2010. Variation in the heat shock response and its implication for predicting the effects of global climate change on species biogeographical distribution ranges and metabolic costs. J. Exp. Biol. 213, 971–979.
Tomanek, L., 2011. Environmental proteomics: changes in the proteome of marine organisms in response to environmental stress, pollutants, infection, symbiosis and development. Annu. Rev. Marine Sci. (available online).
Tomanek, L., Zuzow, M.J., 2010. The proteomic response of the mussel congeners *Mytilus galloprovincialis* and *M. trossulus* to acute heat stress: implications for thermal tolerance limits and metabolic costs of thermal stress. J. Exp. Biol. 213, 3559–3574.
Tyrrell, L., 1991. UV-A (320–380 nm) Radiation as an oxidative stress. In: Sies, H. (Ed.), Oxidative Stress: Oxidants and Antioxidants. Academic Press, San Diego, CA, pp. 57–83.
United Nations Environment Programme, Environmental Effects Assessment Panel, 2005. Environmental effects of ozone depletion and its interactions with climate change: progress report, 2004. Photochem. Photobiol. Sci. 22, 177–184.
United Nations Environment Programme, Environmental Effects Assessment Panel, 2006. Environmental effects of ozone depletion and its interactions with climate change: progress report, 2005. Photochem. Photobiol. Sci. 5, 13–24.
Vega Thurber, R., Epel, D., 2007. Apoptosis in early development of the sea urchin, *Strongylocentrotus purpuratus*. Dev. Biol. 303, 336–346.
Verma, R., Chen, S., Feldman, S., Schieltz, D., Yates, J., Dohmen, J., Deshaies, R.J., 2000. Proteasomal proteomics: identification of nucleotide-sensitive proteasome-interacting proteins by mass spectrometric analysis of affinity-purified proteasomes. Mol. Biol. Cell. 11, 3425–3439.
Veselská, R., Janisch, R., 2000. The effects of UV irradiation on changes in cytoskeleton and viability of mouse fibroblasts L929 cell line. Scripta Medica. 73, 393–408.
Williamson, C., Schulze, P., Hargreaves, B., Seva, J., 1994. The impact of short-term exposure to UV-B radiation on zooplankton communities in north temperate lakes. J. Plankton Res. 16, 205–218.
Wong, J., Créton, R., Wessel, G., 2004. The oxidative burst at fertilization is dependent upon activation of the dual oxidase Udx1. Dev. Cell. 7, 801–814.
World Meteorological Organization, 2007. Scientific assessment of ozone depletion 2006-summary. Global Ozone Research Monitoring Project-Report 50.
Zamansky, G.B., Chou, I.N., 1987. Environmental wavelengths of ultraviolet light induce cytoskeletal damage. J. Invest. Dermatol. 89, 606.
Zeitz, L., Ferguson, R., Garfinkel, A., 1968. Radiation-induced effects on DNA synthesis in developing sea urchin eggs. Rad. Res. 34, 200–208.
Zepp, R.G., Callaghan, T.V., Erickson, D.J., 2003. Interactive effects of ozone depletion and climate change on biogeochemical cycles. Photochem. Photobiol. Sci. 2, 51–61.
Zhang, F., Su, K., Yang, X., Bowe, D.B., Paterson, A.J., Kudlow, J.E., 2003. *O*-GlcNAc modification is an endogenous inhibitor of the proteasome. Cell. 115, 715–725.
Zhang, F., Hu, Y., Huang, P., Toleman, C.A., Paterson, A.J., Kudlow, J.E., 2007. Proteasome function is regulated by cyclic AMP-dependent protein kinase through phosphorylation of RPT6. J. Biol. Chem. 282, 22460–22471.